Aurora kinases promote mitotic progression and asymmetric cell division through activation of Polo kinase

Emmanuel Gallaud[1], Aude Pascal[1], Mathieu Métivier[1], Laurent Richard-Parpaillon[1], Vincent Archambault[2] and Régis Giet[1*]

[1] Univ Rennes, CNRS, IGDR (Institut de Génétique et Développement de Rennes) - UMR 6290, F-35000 Rennes, France

[2] Institute for Research in Immunology and Cancer, Université de Montréal, Montréal, QC, Canada.

[*] Corresponding author: regis.giet@univ-rennes1.fr

Abstract

Organ development and integrity requires the maintenance of a defined and restricted pool of dividing stem cells. This process requires the coupling of mitosis progression to the establishment of stem cells polarization and spindle orientation to ensure that they retain the ability to proliferate while their descendant cells do not proliferate excessively. How this coupling occurs is unknown. Here we show that downstream of Aurora kinases, Polo activity levels are crucial for timely mitotic progression independently from the Spindle Assembly Checkpoint (SAC). In addition, Polo functions downstream of Aurora A to ensure cortical polarity and spindle orientation in neural stem cells, thereby preventing excessive cellular proliferation in developing larval brains, and suppressing tumor development. In addition, induction of aneuploidy in *polo* mutant brain by inactivation of the SAC leads to an increase in tumor development Altogether, our results reveal that the Aurora-Polo kinase axis is an essential module coupling mitotic progression to asymmetric division in NSCs.

Introduction

Correct chromosome segregation in many cell types depends on the Spindle Assembly Checkpoint (SAC) that delays Cyclin B degradation and anaphase onset until all kinetochores are properly attached to spindle microtubules. As a consequence, ablation of SAC genes in dividing cancer cells induces premature anaphase onset and chromosome segregation defects [1–5]. In *aurA* mutant NSCs, mitosis is prolonged and it was initially thought that this effect was due to activation of the SAC[6,7]. Consistent with this idea, these cells are delayed in assembling a functional bipolar spindle and Cyclin B-Cdk1 levels persist longer than normal. However, SAC ablation in *aurA* mutant does not restore normal mitotic progression nor lead to severe aneuploidy; indicating that the prolonged time in mitosis does not result from SAC activation in *aurA* mutants[4]. Thus, despite increased knowledge in the control of mitotic

38 progression, how Aurora A kinase regulates this aspect remains elusive. A possible
39 downstream target is Polo kinase, which is known to be activated by Aurora A and Aurora
40 B[8–13]. In addition, other reports have suggested that Polo kinase contributes to mitotic exit by
41 phosphorylation of several subunits of the APC/C (Anaphase Promoting
42 Complex/Cyclosome), which triggers Cyclin B degradation and anaphase[14–20]. Moreover
43 mitosis is also prolonged in Polo-depleted *Drosophila* S2 cells[21].

44 In the fly NSCs, polarization of the apical cortex is an essential step that ensures asymmetric
45 localization of PAR proteins at the apical cortex and cell fate determinants at the basal cortex.
46 After mitotic spindle alignment along the apico-basal axis and cytokinesis, one cell retains the
47 NSC proliferation fate while the other cell (GMC for Ganglion Mother Cell) inherits the cell
48 fate determinants anchored at the basal cortex and is subjected to differentiation (reviewed in
49 [22]). Both AurA and Polo are needed for cell polarization and for mitotic spindle alignment[23–
50 27]. As a consequence, the two daughter cells acquire the NCS proliferative fate in *aurA* and
51 *polo* mutants and a strong increase of NSC-like population occurs leading to tumor formation
52 in *aurA* and *polo* mutant neural tissues. Therefore, in the context of central brain
53 development, *aurA* and *polo* genes are both tumor suppressors[23,24,27]. Altogether, the
54 contributions of a potential cascade linking Aurora A and Polo kinases ([28] for review) to the
55 control of time in mitosis, spindle orientation, cell polarization and their consequences for
56 tissue development remains unknown. In the context of the stem-cell based *Drosophila*
57 central brain development, we show here that these key features of NSCs are mainly regulated
58 by the activation of Polo by Aurora A and Aurora B.

59 ***polo* mutants NSCs exhibit a SAC-independent mitotic delay.**

60 We first wished to determine if Polo activity promotes mitotic progression in NSCs
61 independently from its role in ensuring correct spindle assembly and chromosome
62 attachments in mitosis. To this end, we examined how time in mitosis was regulated in

63 different *polo* mutants associated with a loss of the SAC (*polo,mad2*^{P}). Western blotting
64 analyses of brain tissues confirmed the absence of Mad2 in the double mutants (Figure 1A).
65 Using time lapse-imaging microscopy, we found that the weak *polo*^{1}/*polo*^{10} and *polo*^{1}/*polo*^{9}
66 hypomorphic mutants showed a prolonged mitosis that was mostly SAC-independent (Figure
67 1B and C). The time in mitosis was strongly increased in strong hypomorphic *polo*^{9}/*polo*^{10}
68 mutants but, by contrast to weak *polo* hypomorphs, ablation of the SAC decreased the time in
69 mitosis, indicating a higher SAC contribution to mitotic delay in strong *polo* mutants. These
70 results were confirmed by analyses of the delay between SAC silencing (as detected by the
71 loss of GFP::Mad2 at kinetochores) and anaphase onset in weak and strong *polo* mutants.
72 This time was 0.8 min in controls, 2.1 to 2.4 min in *polo*^{1}/*polo*^{10} and *polo*^{1}/*polo*^{9} and 8.6 min
73 in *polo*^{9}/*polo*^{10} NSCs. This result reveals that weak interference with Polo kinase prolonged
74 mitosis in a mostly SAC-independent manner but stronger decrease in Polo kinase activity
75 triggers a mitotic delay that is also due to SAC activation. Altogether, these results indicate
76 that the SAC is satisfied well before anaphase onset and cannot account for the prolonged
77 mitosis of *polo* mutant NSCs, similarly to *aurA* mutant NSCs[4].

78 **Constitutively active Polo partially rescues mitotic delays in *polo* and *aurA* mutants.**

79 In human cells, the activation of Plk1 is triggered by the phosphorylation of the Thr210
80 residue in its activation loop by Aurora A[8–10,28]. Therefore, we wondered if this Aurora A-
81 mediated activation of Polo kinase was conserved in the fly and could also regulate the time
82 in mitosis in NSCs. We hypothesized that the expression of a constitutively active Polo kinase
83 (Polo^{T182D} in flies) should decrease the duration of mitosis in *aurA* mutants. In order to test
84 this idea, we generated transgenic flies allowing the expression of different GFP-tagged
85 variants of Polo kinase in brain tissues including wild-type (Polo^{WT}), kinase-dead (Polo^{K54M}),
86 constitutively active (Polo^{T182D}) and constitutively inactive (Polo^{T182A}). We first analyzed the
87 functionality of Polo::GFP variants in NSCs. Their localization was similar to what was

88 previously observed in early embryos and S2 cells (Figure S1 and [29]). Moreover, only
89 Polo^{WT}::GFP was able to restore viability of the strong *polo*$^{9/10}$ hypomorph (hereafter referred
90 to as *polo* mutant) when expressed under the control of a ubiquitous Actin5C promoter
91 (Figure 2A-B). We then assayed the ability of each of these variants to reduce the time in
92 mitosis of *polo* NCSs by live microscopy (Figure 2C-D). Expression of Polo^{T182D}, Polo^{T182A}
93 and Polo^{K54M} in a WT background slightly increased the time in mitosis of NSCs when
94 compared to the expression of Polo^{WT}, suggesting hypermorphic or dominant-negative
95 effects. Moreover, only expression of Polo^{WT} was able to restore a normal time in mitosis
96 when expressed in *polo* mutants (8.0 vs 45.6 min). Interestingly, expression of the Polo^{T182D}
97 variant decreased by more than half the time in mitosis of *polo* mutant NSCs. Given the
98 literature, we envisaged that the excess of Polo kinase activity in WT and *polo* mutant cells
99 may perturb kinetochore attachments to spindle microtubules and activate the SAC[30–34]. We
100 therefore decided to examine the time in mitosis of NSCs upon Polo^{T182D} expression, in
101 *mad2*^{P} mutant and *polo,mad2*^{P} double mutant. Interestingly, the increased time in mitosis
102 resulting from Polo^{T182D} expression in WT cells was not abrogated following deletion of the
103 SAC, indicating that this delay did not result from aberrant kinetochore attachments.
104 However, expression of Polo^{T182D} was able to reduce by 34.2% the time in mitosis in
105 *polo,mad2*^{P} double mutant NSCs. These results suggest that Polo^{T182D} is not a fully functional
106 protein, in agreement with a previous study in human cells[32]. Finally, the ability of Polo^{T182D}
107 to delay mitotic exit (anaphase entry) in a SAC-independent manner (in WT NSCs) while
108 accelerating mitotic exit in *polo,mad2*^{P} double mutants, suggests that Polo activation levels
109 must be finely controlled to set the normal duration of mitosis.

110 To investigate if the mitotic delay observed in *aurA* and in *aurA,mad2*^{P} mutants was Polo-
111 kinase-dependent, we expressed Polo^{WT} and Polo^{T182D} in these backgrounds (Figure 3A-B and
112 S2A). We found that expression of Polo^{WT} and Polo^{T182D} decreased the time in mitosis of

113 *aurA* and *aurA,mad2*^{P} mutants NSCs, suggesting that Polo kinase T182 phosphorylation by
114 Aurora A contributes to mitotic exit.

115 **AurA and Ial are both required for Polo-dependent mitotic progression.**

116 The mitotic phosphorylation of Polo on T182 is also mediated by Aurora B kinase/Ial (Ipl1-
117 Aurora-like in flies), a component of the Chromosome Passenger Complex (CPC) at
118 centromeres and during cytokinesis[11,12,29]. We therefore wondered if Aurora B was also
119 contributing, with Aurora A, to the control of the time in mitosis through Polo kinase
120 phosphorylation on T182. As described before for *CPC* (*survivin*) mutants, *ial* mutant NSCs
121 displayed prolonged mitosis (9.2 min for *ial*^{2A43}/*ial*^{1689} vs 6.0 min in a control, Figure 3C-D,
122 S2C and [35]). This delay was significantly reduced upon Polo^{T182D} expression (8.5 min)
123 indicating that the mitotic delay in *ial* mutant is partially Polo kinase-dependent. Strikingly,
124 combination of *ial* and *aurA* mutations triggered a synergistic delay in the time in mitosis, as
125 most of the double mutant NSCs failed to exit mitosis after more than 150 min (Figure S2B-
126 C).

127 **Polo and the SAC protect NSCs against aneuploidy and excessive proliferation.**

128 In addition to their role for the control of the time in mitosis, AurA and Polo are both required
129 for cell polarization and mitotic spindle alignment in NSCs[23,24,27]. Thus, we hypothesized that
130 activation of Polo by AurA may partly underly their requirements in the asymmetric division
131 of NSCs. We first analyzed the larval brain phenotypes of the weak and strong *polo*
132 hypomorphs. We found that NSC numbers (Deadpan-positive cells) increased in the central
133 brain of both weak and strong *polo* mutants. Interestingly, ablation of the SAC with the
134 *mad2*^{P} mutation abrogated this increase in a strong *polo* hypomorph but not in weak *polo*
135 hypomorphs (Figure 4A-B). As NSCs proliferation can be perturbed by aneuploidy in flies[4,5],
136 we also monitored the aneuploidy and polyploidy levels of weak and strong *polo* hypomorphs
137 associated with loss of the SAC (Figure 4C-D). We found that 36 to 41% of the mitotic cells

138 in *polo,mad2*^{P} double mutants were either aneuploid or polyploid, indicating that *polo* mutant
139 brain tissues were prone to chromosome segregation errors.

140 To check if the number of NSCs reflects their ability to proliferate, we performed brain
141 transplantation experiments. We transplanted weak or strong *polo* mutant brain tissues in
142 which the SAC was active or not, in the abdomen of host WT flies and monitored the growth
143 of the transplants[36,37]. Surprisingly, inactivation of the SAC and the subsequent increase in
144 aneuploidy correlated with severely enhanced tumor growth of weaker *polo* mutant NSCs
145 (45.1 and 51.5% vs. 22.0 and 24.7% of transplanted flies). SAC inactivation had no effect on
146 strong *polo* tumor growth as it was already close to maximal (85.2 vs. 86.5% of transplanted
147 flies) (Figure 4E-F). These results suggest that Polo collaborates with the SAC to protect
148 NSCs against chromosome segregation errors and excessive proliferation. In this way, Polo is
149 akin to a tumor suppressor.

150 **AurA-dependent tumor suppression is largely mediated by Polo.**

151 Given that Polo and AurA both act like tumor suppressors in NSCs, we decided to investigate
152 if the tumor suppression potential of *aurA* mutants was Polo-dependent. We therefore
153 expressed a Polo^{T182D} kinase in an *aurA* mutant background and quantified the number of
154 NSCs in the central brain region. Consistent with several studies[4,23,27], the NSC number in
155 *aurA* mutants was increased 10-25 times compared to control brains (2050 NSCs per lobe,
156 Figure 5 A-B). Strikingly, while expression of Polo^{T182D} had no effect on its own (95 NSCs
157 per lobe), it was sufficient to strongly diminish the NSC amplification incurred in *aurA*
158 mutant tissues (390 NSCs). We also compared tumor growth progression after transplantation
159 of *aurA* mutant neural tissues expressing or not Polo^{T182D} (Figure 5C-D). We found that 90%
160 of transplanted *aurA* mutant brain tissues labeled with mCherry produced large tumors that
161 killed host flies after 15 days. When Polo^{T182D} was expressed in *aurA* mutant, only 10 % and
162 55 % of the injected hosts developed tumors after 15 and 30 days respectively, indicating that

163 the tumor suppressor potential of AurA is Polo-kinase dependent (Figure 5D). Importantly,
164 the ploidy defects caused by *aurA* mutation (11.8% of the cells) were unchanged following
165 Polo^{T182D} expression (13.1% of the cells), ruling out differences in ploidy as the cause of the
166 *aurA* mutant tumor growth restriction by Polo^{T182D} (Figure 5E).

167 Aurora A is required to regulate larval brain development by controlling mitotic spindle
168 orientation and cell polarization in NSC asymmetric division [23,25–27]. We therefore analyzed
169 these two processes in *aurA* mutant NSCs expressing Polo^{T182D}. We first monitored NSC
170 polarization by analyzing the localization of aPKC and Miranda apical and basal crescents
171 respectively. We found that both aPKC and Miranda crescents were properly localized in 100
172 % of control or Polo^{T182D} expressing NSCs. By contrast and in agreement with previous
173 reports, most *aurA* mutant NSCs (78%) displayed abnormally weak homogenous cortical
174 aPKC while Miranda was properly localized at the basal cortex (Figure 5F-H). Strikingly,
175 expression of Polo^{T182D} in *aurA* mutant restored the presence of the aPKC apical crescent in
176 84% of the NCSs. In parallel, we also measured mitotic spindle alignment along the apico-
177 basal axis in *aurA* mutant with or without Polo^{T182D} expression. In control and Polo^{T182D}
178 expressing NSCs, the vast majority of mitotic spindles were properly oriented in metaphase
179 (angle < 30°: 94% and 100%) while *aurA* mutant NSCs displayed a random mitotic spindle
180 alignment (angle < 30°: 41.8%) in agreement with previous reports [23,27]. Strikingly, Polo^{T182D}
181 expression was sufficient to significantly restore the *aurA* mutant-dependent spindle
182 alignment defects (angle < 30°: 76.3%; Figure 5F, I and J). Altogether, these results indicate
183 that Polo functions downstream of AurA to ensure the asymmetry of NSC divisions that is
184 required to prevent their excessive proliferation during larval brain development.

185 The regulation of the time in mitosis is a complex process that is regulated by the
186 maintenance of Cyclin-CDK activity, satisfaction of the SAC and activation of the APC/C by
187 phosphorylation/dephosphorylation events[17–20] ([38] for review). Here we present several

188 evidence supporting the idea that the Aurora-Polo signaling cascade is pivotal to control the
189 duration of mitosis. Firstly, the loss of Aurora A or Aurora B leads to a synergistic extension
190 of the time in mitosis, much like inactivation of Polo. This mitotic delay can be rescued by the
191 expression of a constitutively active $Polo^{T182D}$, consistent with the idea that Aurora-dependent
192 phosphorylation of Polo at T182 is the underlying connection. Interestingly, the use of weak
193 or strong hypomorphic *polo* mutants and the controlled expression of a dominant $Polo^{T182D}$
194 active kinase allowed to establish the importance of Polo kinase activity thresholds. We found
195 that weak *polo* hypomorphs are characterized by near normal spindle formation and a
196 prolonged mitosis in which the SAC has little if no contribution. By contrast, strong *polo*
197 hypomorphs exhibit spindle defects associated with a prolonged mitosis that is partially SAC-
198 independent. The use of active $Polo^{T182D}$ has enabled us to highlight the subversive function
199 of Polo kinase in the control of the time in mitosis. Indeed, when expressed in a wild type
200 background, $Polo^{T182D}$ significantly lengthens mitosis whereas it shortens it in a null genetic
201 background (Figure 2D-E, Figure 3B and D and [33]). This apparent antagonism could be
202 explained by the fact that Polo inhibits the APC/C activator Cdc20 when the SAC is
203 unsatisfied but is also necessary to activate the phosphorylation of APC/C subunits and thus
204 the exit from mitosis[19,20,39].

205 This work also is first to demonstrate the essential role of the activation of Polo kinase by
206 Aurora A for the orientation of the mitotic spindle and the polarization of neural stem cells.
207 We show here that tumor growth of *aurA* mutant brains is strongly inhibited by the persistent
208 activation of Polo. This restoration of tissue homeostasis is likely caused by the almost
209 complete rescue of *aurA* mutant cell polarity defects following constant Polo activation.
210 Given that a past study showed that Aurora A phosphorylation of the PAR complex is the
211 main player leading to cell polarization at least *in vitro*[25], we speculate that yet

212 uncharacterized Polo-dependent phosphorylation of cortical or polarity proteins are also
213 essential to mediate NSC polarization.

214 In addition, rescue of tissue homeostasis by Polo^{T182D} may also be mediated by a direct
215 regulation of the spindle orientation machinery by Polo together with Aurora A[26] or by
216 stimulation of centrosomal microtubule nucleation and interaction with the cell cortex ([13,40]
217 and [41] for review). In conclusion, this work has revealed that essential characteristics of
218 NSCs, such as the duration of mitosis and cell polarization, are in fact regulated by a signaling
219 cascade leading to the spatio-temporal activation of the Polo protein kinase by the Aurora
220 kinases, with a profound impact on tissue development. Further studies will be required to
221 identify and investigate the functions of the Polo targets in these essential processes.
222

Acknowledgements:

This work was supported by Fondation pour la Recherche Médicale (DEQ20170336742). We thank members of the "Cytoskeleton and Cell Proliferation" lab as well as Roland Le Borgne and Damien Coudreuse for helpful discussions. We are grateful to Renata Basto for advices on tumor growth assays, Clemens Cabernard, David Sharp, Juliette Mathieu and Jean-René Huynh for antibodies, flies and plasmids. We also acknowledge Stéphanie Dutertre and Xavier Pinson for their help using the microscopes of the Microscopy Rennes imaging center facility (MRic).

Author Contributions:

R.G. and E.G. conceived the project. E.G. performed experiments and quantifications with the help of L.R.-P. (Figure 4E-F), A.P. (Figure 2A), R.G. (Figure 1D-E, Figure 4A-D) and M.M. (initial experiment corresponding to Figure 3A-B). R.G. and E.G. discussed the data and wrote the manuscript with the help of V.A.

Competing Interests statement:

The authors declare no competing interests.

Data availability:

Numerical data are available in the Table S1 and all other data are available upon request.

240 **References**

241 1. Dominguez-Brauer, C. *et al.* Targeting Mitosis in Cancer: Emerging Strategies. *Mol.*
242 *Cell* **60**, 524–536 (2015).
243 2. Janssen, A., Kops, G. J. P. L. & Medema, R. H. Elevating the frequency of
244 chromosome mis-segregation as a strategy to kill tumor cells. *Proc. Natl. Acad. Sci.* **106**,
245 19108–19113 (2009).
246 3. Silk, A. D. *et al.* Chromosome missegregation rate predicts whether aneuploidy will
247 promote or suppress tumors. *Proc. Natl. Acad. Sci.* **110**, E4134–E4141 (2013).
248 4. Caous, R. *et al.* Spindle assembly checkpoint inactivation fails to suppress neuroblast
249 tumour formation in aurA mutant Drosophila. *Nat. Commun.* **6**, (2015).
250 5. Gogendeau, D. *et al.* Aneuploidy causes premature differentiation of neural and
251 intestinal stem cells. *Nat. Commun.* **6**, 8894 (2015).
252 6. Glover, D. M., Leibowitz, M. H., McLean, D. A. & Parry, H. Mutations in aurora
253 prevent centrosome separation leading to the formation of monopolar spindles. *Cell* **81**, 95–
254 105 (1995).
255 7. Giet, R. *et al.* Drosophila Aurora A kinase is required to localize D-TACC to
256 centrosomes and to regulate astral microtubules. *J. Cell Biol.* **156**, 437–451 (2002).
257 8. Macůrek, L. *et al.* Polo-like kinase-1 is activated by aurora A to promote checkpoint
258 recovery. *Nature* **455**, 119–123 (2008).
259 9. Seki, A., Coppinger, J. A., Jang, C.-Y., Iii, J. R. Y. & Fang, G. Bora and the Kinase
260 Aurora A Cooperatively Activate the Kinase Plk1 and Control Mitotic Entry. *Science* **320**, 5
261 (2008).
262 10. Bruinsma, W., Macůrek, L., Freire, R., Lindqvist, A. & Medema, R. H. Bora and
263 Aurora-A continue to activate Plk1 in mitosis. *J. Cell Sci.* 11 (2014).
264 11. Carmena, M. *et al.* The Chromosomal Passenger Complex Activates Polo Kinase at
265 Centromeres. *PLoS Biol.* **10**, 15 (2012).
266 12. Kachaner, D. *et al.* Interdomain allosteric regulation of Polo kinase by Aurora B and
267 Map205 is required for cytokinesis. *J. Cell Biol.* **207**, 201–211 (2014).
268 13. Joukov, V., Walter, J. C. & De Nicolo, A. The Cep192-Organized Aurora A-Plk1
269 Cascade Is Essential for Centrosome Cycle and Bipolar Spindle Assembly. *Mol. Cell* **55**, 578–
270 591 (2014).
271 14. Shirayama, M., Zachariae, W., Ciosk, R. & Nasmyth, K. The Pololike kinase Cdc5p
272 and the WDrepeat protein Cdc20p/fizzy are regulators and substrates of the anaphase
273 promoting complex in Saccharomyces cerevisiae. *EMBO J.* **17**, (1998).
274 15. Descombes, P. & Nigg, E. A. The pololike kinase Plx1 is required for M phase exit
275 and destruction of mitotic regulators in Xenopus egg extracts. *EMBO J.* **17**, (1998).
276 16. Charles, J. F., Jaspersen, S. L., Tinker-Kulberg, R. L., Hwang, L. & Morgan, D. O.
277 The Polo-related kinase Cdc5 activates and is destroyed by the mitotic cyclin destruction
278 machinery in S. cerevisiae. *Curr. Biol.* **8**, (1998).
279 17. Golan, A., Yudkovsky, Y. & Hershko, A. The Cyclin-Ubiquitin Ligase Activity of
280 Cyclosome/APC Is Jointly Activated by Protein Kinases Cdk1-Cyclin B and Plk. *J. Biol.*
281 *Chem.* **277**, (2002).
282 18. Kraft, C. *et al.* Mitotic regulation of the human anaphase-promoting complex by
283 phosphorylation. *EMBO J.* **22**, 6598–6609 (2003).
284 19. Qiao, R. *et al.* Mechanism of APC/CCDC20 activation by mitotic phosphorylation.
285 *Proc. Natl. Acad. Sci.* **113**, 9 (2016).
286 20. Zhang, S. *et al.* Molecular mechanism of APC/C activation by mitotic
287 phosphorylation. *Nature* **533**, 19 (2016).
288 21. Conde, C. *et al.* Drosophila Polo regulates the spindle assembly checkpoint through

289 Mps1dependent BubR1 phosphorylation. *EMBO J.* **32**, (2013).
290 22. Gallaud, E., Pham, T. & Cabernard, C. Drosophila melanogaster Neuroblasts: A
291 Model for Asymmetric Stem Cell Divisions. in *Asymmetric Cell Division in Development,*
292 *Differentiation and Cancer* (eds. Tassan, J.-P. & Kubiak, J. Z.) vol. 61 183–210 (Springer
293 International Publishing, 2017).
294 23. Wang, H. *et al.* Aurora-A acts as a tumor suppressor and regulates self-renewal of
295 Drosophila neuroblasts. *Genes Dev.* **20**, 3453–3463 (2006).
296 24. Wang, H., Ouyang, Y., Somers, W. G., Chia, W. & Lu, B. Polo inhibits progenitor
297 self-renewal and regulates Numb asymmetry by phosphorylating Pon. *Nature* **449**, 96–100
298 (2007).
299 25. Wirtz-Peitz, F., Nishimura, T. & Knoblich, J. A. Linking Cell Cycle to Asymmetric
300 Division: Aurora-A Phosphorylates the Par Complex to Regulate Numb Localization. *Cell*
301 **135**, 161–173 (2008).
302 26. Johnston, C. A., Hirono, K., Prehoda, K. E. & Doe, C. Q. Identification of an Aurora-
303 A/PinsLINKER/ Dlg Spindle Orientation Pathway using Induced Cell Polarity in S2 Cells.
304 *Cell* **138**, 1150–1163 (2009).
305 27. Lee, C.-Y. *et al.* Drosophila Aurora-A kinase inhibits neuroblast self-renewal by
306 regulating aPKC/Numb cortical polarity and spindle orientation. *Genes Dev.* **20**, 3464–3474
307 (2006).
308 28. Joukov, V. & Nicolo, A. D. Aurora-PLK1 cascades as key signaling modules in the
309 regulation of mitosis. *Sci. Signal.* 26 (2018).
310 29. Kachaner, D. *et al.* Coupling of Polo kinase activation to nuclear localization by a
311 bifunctional NLS is required during mitotic entry. *Nat. Commun.* **8**, (2017).
312 30. Foley, E. A., Maldonado, M. & Kapoor, T. M. Formation of stable attachments
313 between kinetochores and microtubules depends on the B56-PP2A phosphatase. *Nat. Cell*
314 *Biol.* **13**, (2011).
315 31. Beck, J. *et al.* Ubiquitylation-dependent localization of PLK1 in mitosis. *Nat. Cell*
316 *Biol.* **15**, (2013).
317 32. Paschal, C. R., Maciejowski, J. & Jallepalli, P. V. A stringent requirement for Plk1
318 T210 phosphorylation during K-fiber assembly and chromosome congression. *Chromosoma*
319 **121**, (2012).
320 33. Barbosa, J. *et al.* Polo regulates Spindly to prevent premature stabilization of
321 kinetochore–microtubule attachments. *EMBO J.* **39**, (2020).
322 34. Liu, D., Davydenko, O. & Lampson, M. A. Polo-like kinase-1 regulates kinetochore–
323 microtubule dynamics and spindle checkpoint silencing. *J. Cell Biol.* **198**, 491–499 (2012).
324 35. Mathieu, J. *et al.* Aurora B and Cyclin B Have Opposite Effects on the Timing of
325 Cytokinesis Abscission in Drosophila Germ Cells and in Vertebrate Somatic Cells. *Dev. Cell*
326 **26**, 250–265 (2013).
327 36. Caussinus, E. & Gonzalez, C. Induction of tumor growth by altered stem-cell
328 asymmetric division in Drosophila melanogaster. *Nat. Genet.* **37**, 1125–1129 (2005).
329 37. Castellanos, E., Dominguez, P. & Gonzalez, C. Centrosome Dysfunction in
330 Drosophila Neural Stem Cells Causes Tumors that Are Not Due to Genome Instability. *Curr.*
331 *Biol.* **18**, 1209–1214 (2008).
332 38. Corbett, K. D. Molecular Mechanisms of Spindle Assembly Checkpoint Activation
333 and Silencing. in *Centromeres and Kinetochores* (ed. Black, B. E.) vol. 56 429–455 (Springer
334 International Publishing, 2017).
335 39. Jia, L., Li, B. & Yu, H. The Bub1–Plk1 kinase complex promotes spindle checkpoint
336 signalling through Cdc20 phosphorylation. *Nat. Commun.* **7**, 10818 (2016).
337 40. Conduit, P. T. *et al.* The Centrosome-Specific Phosphorylation of Cnn by Polo/Plk1
338 Drives Cnn Scaffold Assembly and Centrosome Maturation. *Dev. Cell* **28**, 659–669 (2014).

41. Magnaghi-Jaulin, L., Eot-Houllier, G., Gallaud, E. & Giet, R. Aurora A Protein Kinase: To the Centrosome and Beyond. *Biomolecules* **9**, 28 (2019).

343 **Figures**

344 **Figure 1: *polo* mutant NSCs display a SAC-independent mitotic delay.**

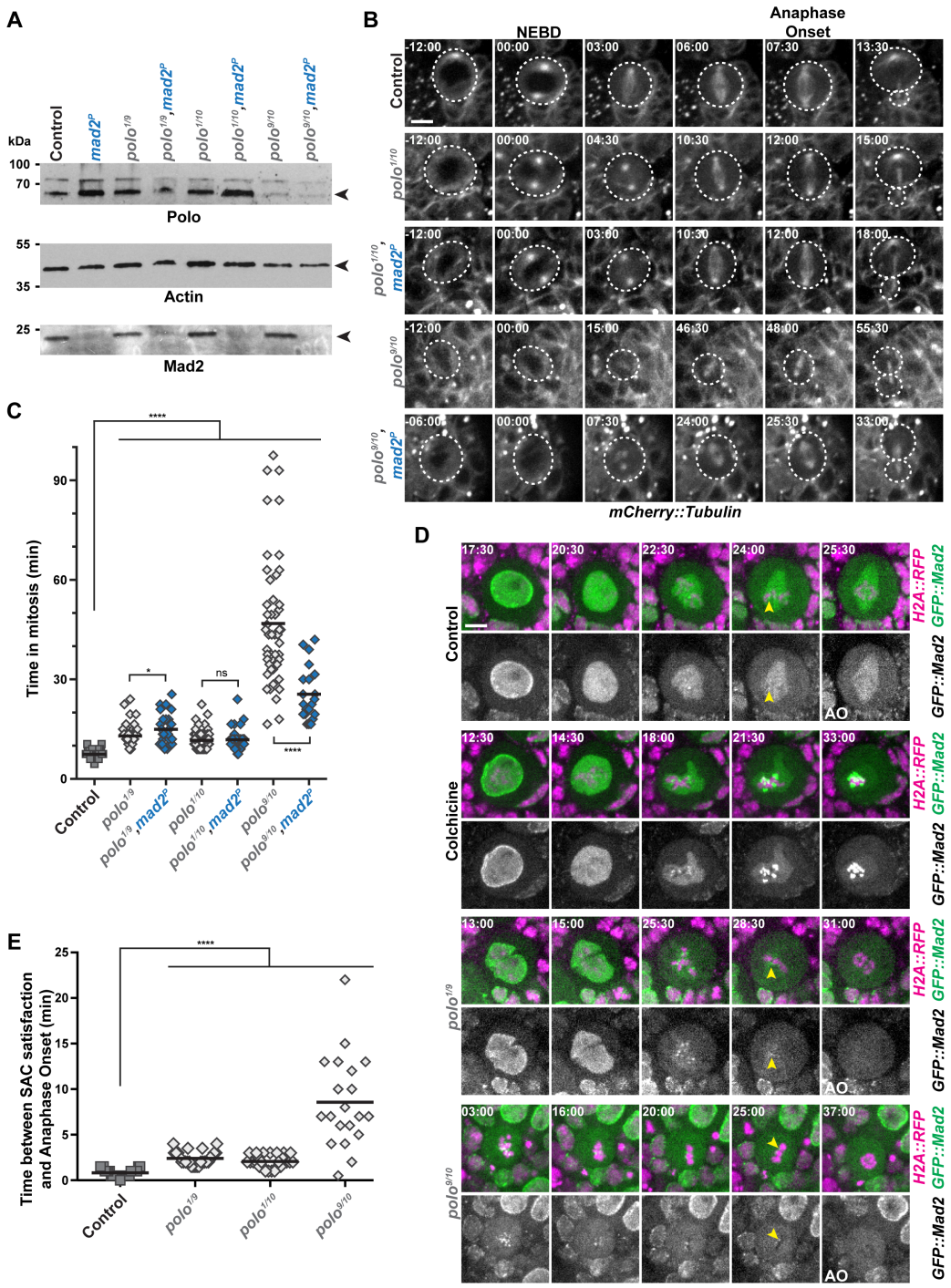

345 **Figure 1**

346 **A)** Polo, Mad2 and Actin Western blot analyses in *polo* and *polo,mad2^{P}* mutant brain extracts.

347 The genotypes are indicated for each lane. *polo^{1}/polo^{10}* and *polo^{1}/polo^{9}* are weak hypomorphs

348 and *polo^{9}/polo^{10}* is a strong hypomorph. **B)** Time-lapse imaging of mitosis in *polo* mutants in

349 the absence or presence of Mad2. Selected image series of dividing NSCs of the indicated
350 genotypes expressing mCherry::Tubulin (from top to bottom). The white dashed line outlines
351 the dividing NSCs. Scale bar: 5 μm. Time is min:s (t=00:00 is NEBD). **C)** Quantification of
352 time in mitosis from NEBD to anaphase onset for NSCs of the indicated genotypes. Means
353 are shown as black bars. Mann-Whitney unpaired test: ns: $p>0.05$; *: $p<0.05$; ****: $p<0.0001$.
354 **D)** GFP::Mad2 kinetochore localization in control, colchicine-treated, and *polo* mutant NCSs
355 expressing His2Av::mRFP1. Colchicine treatment (20μM) was used as a control for
356 GFP::Mad2 accumulation on kinetochores. Yellow arrowheads indicate the last kinetochore
357 labelled with GFP::Mad2 before anaphase onset (AO). Scale bar: 5 μm. Time is min:s
358 (t=00:00 is the beginning of the experiment). **E)** Quantification of the time between SAC
359 satisfaction (disappearance of the last GFP::Mad2-labeled kinetochores) and anaphase onset
360 in NSCs of the indicated genotypes. Means are shown as black bars. Mann-Whitney unpaired
361 test: ****: $p<0.0001$. Numerical data (mean, SD and *n*) are available in Table S1.
362

363 **Figure 2: Loss or excess of Polo activity is not compatible with normal mitosis duration**

364 **and *Drosophila* viability.**

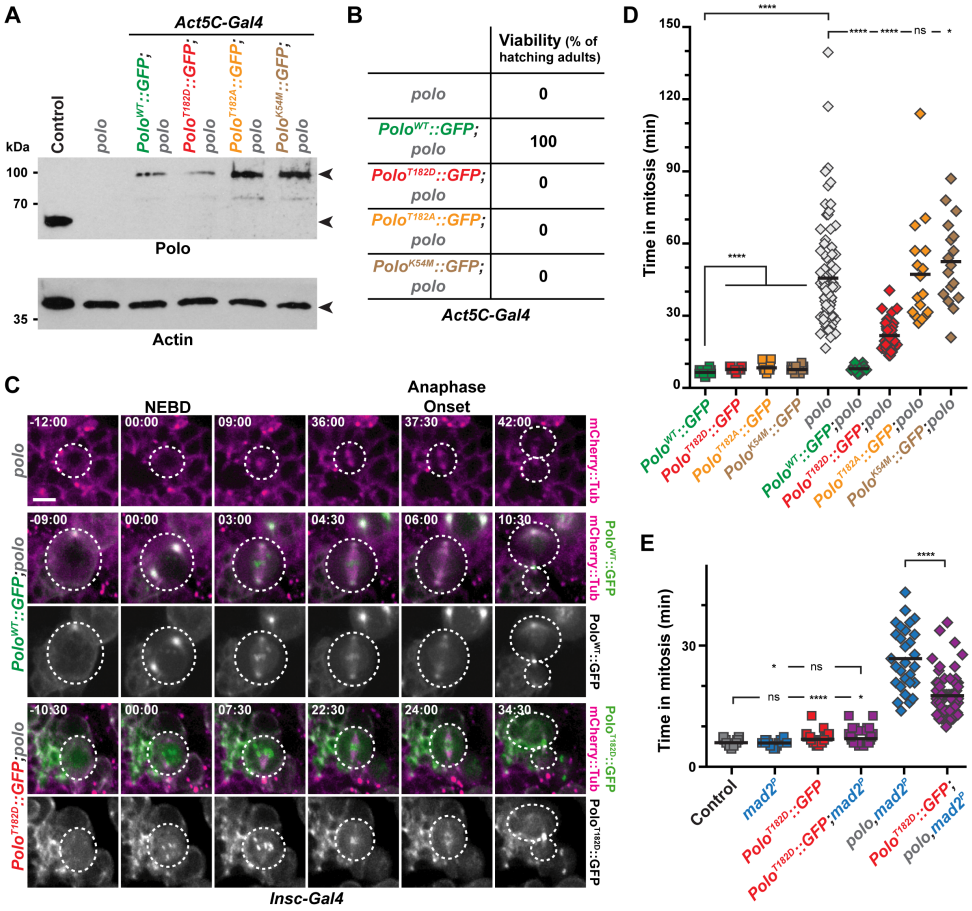

365 **Figure 2**

366 **A)** Polo and Actin Western blot analyses showing the expression of endogenous Polo kinase

367 in control and GFP-tagged Polo variants (WT, T182D, T182A and K54M) expressed

368 ubiquitously in *polo* mutant brains. The genotypes are indicated for each lane. Actin was used

369 as a loading control. **B)** Hatching rates of *polo* mutants expressing the indicated Polo variants.

370 **C)** Time-lapse imaging of mitosis in *polo* mutant NSCs expressing the indicated Polo variants

371 and mCherry::Tubulin. The white dashed lines outline the dividing NSCs. Scale bar: 5 µm.

372 Time is min:s (t=00:00 is NEBD). **D-E)** Quantification of the time in mitosis of NSCs of the

373 indicated genotypes. Means are shown as black bars. Mann-Whitney unpaired test: ns:

374 p>0.05; *: $p<0.05$; ****: $p<0.0001$. Numerical data (mean, SD and *n*) are available in Table

375 S1.

376 **Figure 3: Mitotic delays in *aurA* and *aurB* mutants are Polo-dependent.**

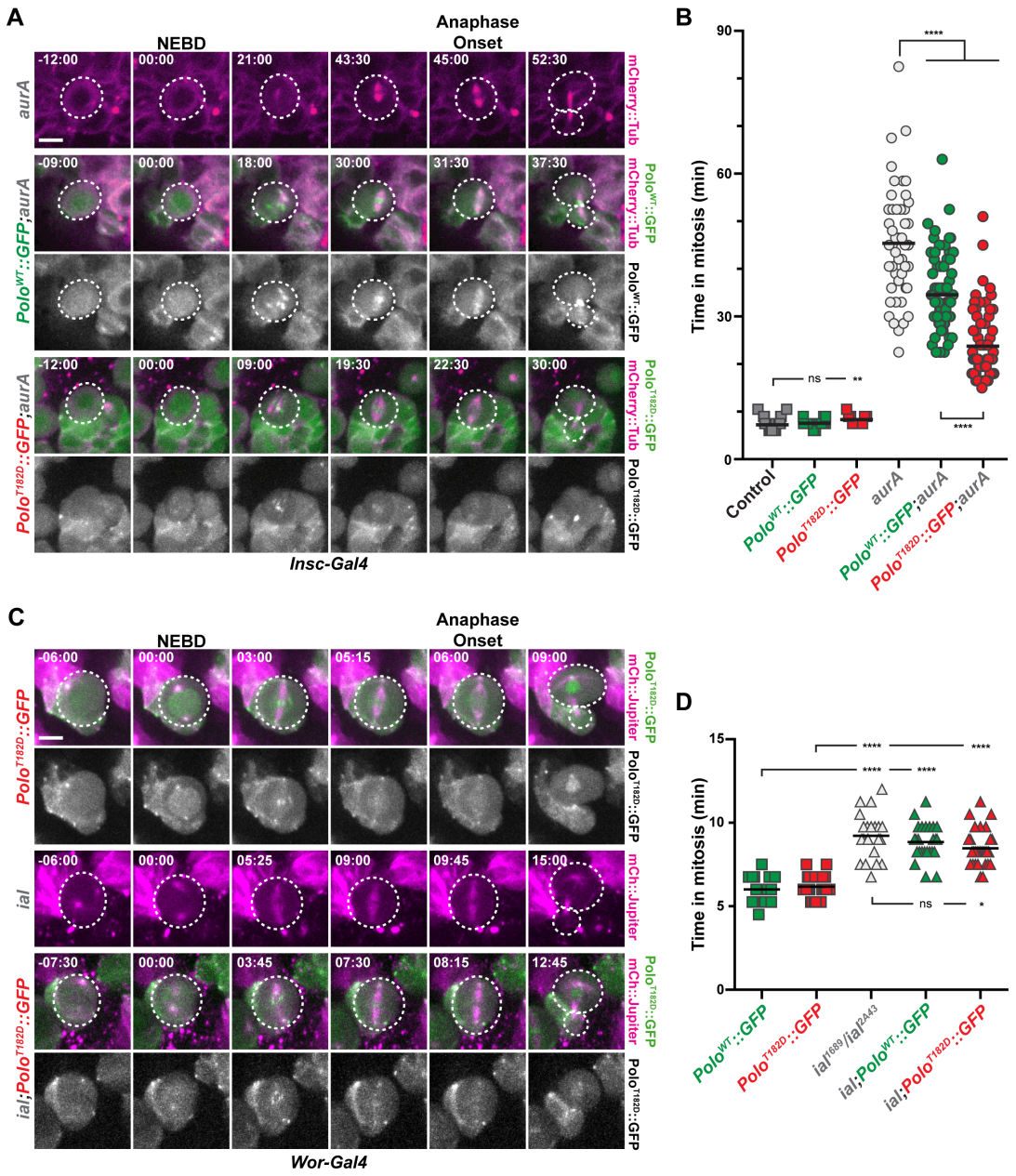

377 **Figure 3**

378 **A, C)** Time-lapse imaging of mitosis in *aurA* and *aurB/ial* mutant NSCs expressing the
379 indicated Polo variants and mCherry::Tubulin. The white dashed lines outline the dividing
380 NSCs. Scale bar: 5 µm. Time is min:s (t=00:00 is NEBD). **B, D)** Quantification of time in
381 mitosis for the indicated genotypes. Means are shown as black bars. Mann-Whitney unpaired
382 tests: ns: $p>0.05$; *: $p<0.05$; **: $p<0.01$; ****: $p<0.0001$. Numerical data (mean, SD and n)
383 are available in Table S1.

384 **Figure 4: Impairing the SAC in *polo* mutants induces aneuploidy and promotes tumor**

385 **growth.**

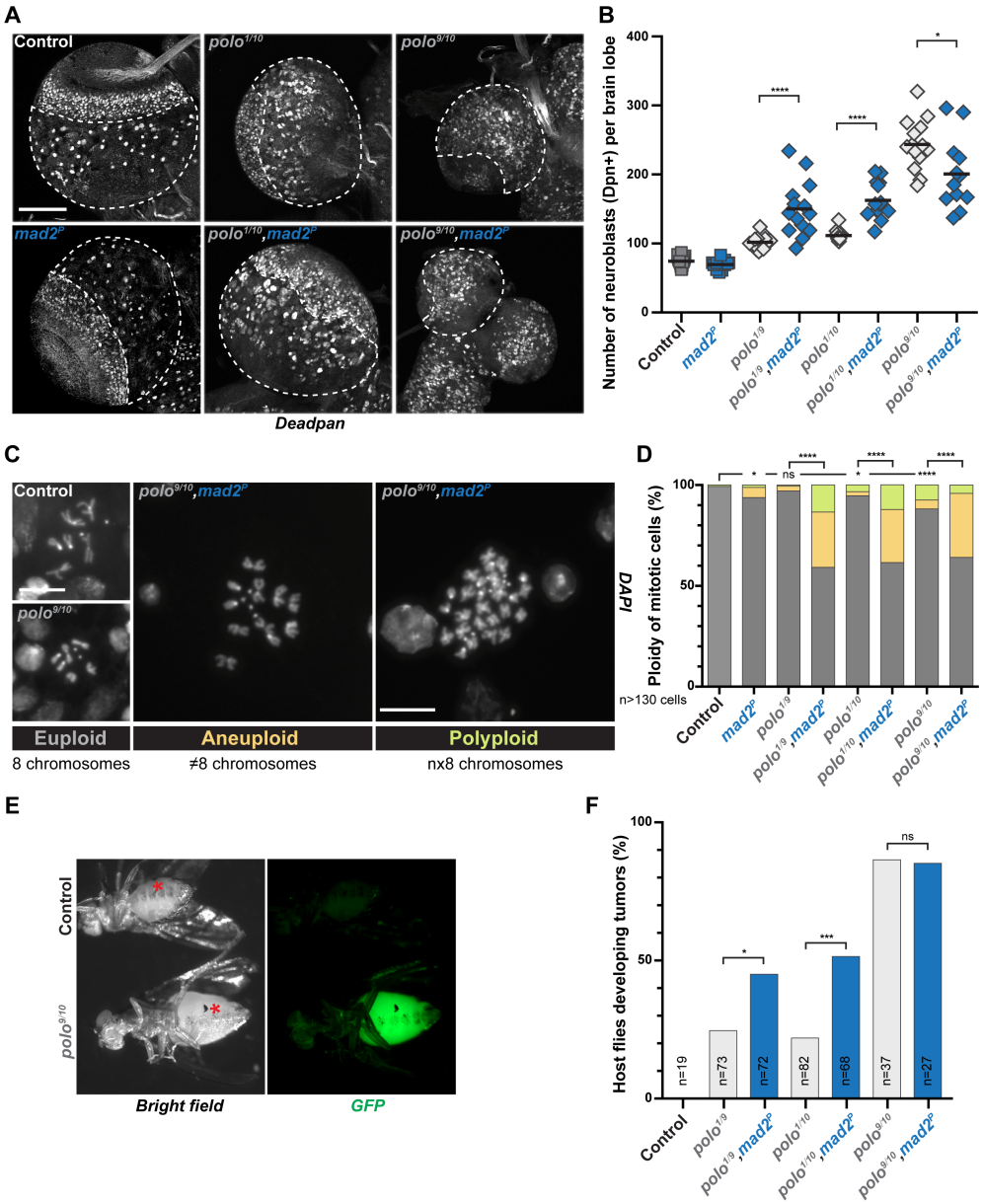

386 **Figure 4**

387 **A)** Representative images of larval brain lobes of the indicated genotypes stained for the NSC

388 marker Deadpan. The white dashed lines outline the central brain area where NSCs were

389 scored. Note the reduced brain lobe size in the *polo*$^{9/10}$ mutant. Scale bar: 100 µm. **B)**

390 Quantifications of Deadpan-positive NSCs per brain lobe for the indicated genotypes. Mann-

391 Whitney unpaired test: *: $p<0.05$; ****: $p<0.0001$. Means are shown in black. **C)**

392 Representative images of the three classes of mitotic figures observed from squashed brains

393 stained with DAPI: euploid (8 chromosomes), aneuploid (more or less than 8 chromosomes)
394 and polyploid (multiple of 8 chromosomes) cells. Scale bar: 10 μm. **D)** Percentage of mitotic
395 brain cells with ploidy defects (aneuploidy and polyploidy) for the indicated genotypes. For
396 statistical analyses, the proportion of euploidy was compared to the proportion of ploidy
397 defects. Fisher's exact test: ns: $p>0.05$; *: $p<0.05$; ****: $p<0.0001$. **E)** Examples of wild-type
398 adult host flies 30 and 15 days after transplantation with control and *polo* mutant brain lobe
399 expressing His2Av::GFP as a readout for tumor development (bottom). Asterisks indicate
400 transplantation scars. **F)** Proportion of host flies developing tumors following the
401 transplantation of brain lobes from the indicated genotypes. Fisher's exact test; ns: $p>0.05$; *:
402 $p<0.05$; ***: $p<0.001$. Numerical data (mean, SD and n) are available in Table S1.
403
404

Figure 5: Activation of Polo restores NSCs polarization, spindle orientation and inhibits tumor growth in an *aurA* mutant.

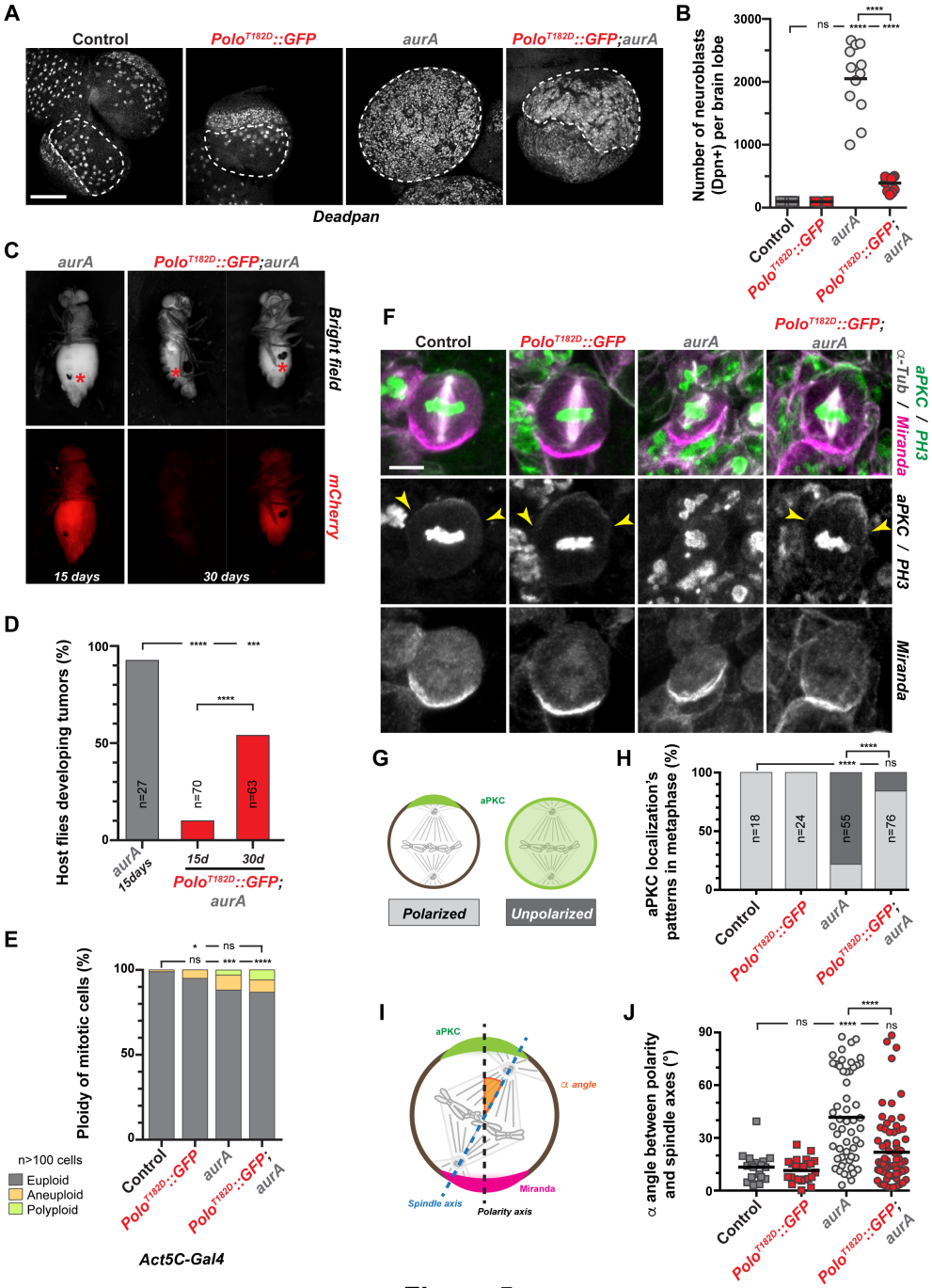

Figure 5

A) Representative images of fixed control and *aurA* mutant larval brain lobes with or without Polo^{T182D}::GFP expression and stained for the NSC marker Deadpan. The white dashed lines outline the central brain area where NSCs were scored. Note that the expression Polo^{T182D} in *aurA* mutant restores the delimitation between the central brain and neuroepithelium. Scale

412 bar: 100 μm. **B)** Quantification of the NSC number in each brain lobe for the indicated
413 genotypes. **C)** Examples of wild-type adult host flies 15 and 30 days after transplantation with
414 *aurA* mutant or *aurA* mutant expressing Polo^{T182D}::GFP brain lobes expressing
415 mCherry::Tubulin as a readout to follow tumor development. Red asterisks indicate
416 transplantation scars. **D)** Percentage of host flies developing tumors 15 and 30 days after the
417 transplantation of brain lobes from the indicated genotypes. **E)** Quantification of ploidy
418 defects scored in neural tissue for the indicated genotypes. **F)** Representative images of
419 control, Polo^{T182D}::GFP, *aurA* mutant and Polo^{T182D}::GFP;*aurA* metaphase NSCs stained for
420 Miranda (magenta in the merge), aPKC and Phospho-Histone H3 (green in the merge), and α-
421 Tubulin (white in the merge). Yellow arrowheads indicate the edges of aPKC crescent. Scale
422 bar: 5 μm. **G)** Schematic representation of aPKC localization patterns observed in NSCs: left:
423 aPKC forms a crescent which defines the apical cortex of the control cell; right: aPKC is
424 unpolarized and exhibits an homogenous cytoplasmic and cortical localization. **H)** Percentage
425 of NSCs of the indicated genotypes with either a polarized apical crescent (light grey) or a
426 homogenous cortical and cytoplasmic aPKC localization (dark grey). **I)** Schematic illustration
427 of the method used to measure the spindle alignment α angle (orange) between the polarity
428 axis (black dashed line), determined by aPKC (green) and Miranda (magenta), and the spindle
429 axis (blue dashed line) determined by spindle poles (See Methods). **J)** Quantification of the
430 α angle between polarity and spindle axes in metaphase NSCs for the indicated genotypes.
431 Mann-Whitney unpaired test: ns: $p>0.05$; ****: $p<0.0001$. Means are shown as black bars.
432 For panels D), E) and H): Fisher's exact test: ns: $p>0.05$; *: $p<0.05$, ***: $p<0.001$, ****:
433 $p<0.0001$. Note that in panel E, the proportion of euploidy was compared to the proportion of
434 ploidy defects for statistical analyses. Numerical data (mean, SD and *n*) are available in Table
435 S1.
436

Materials and Methods

Fly strains and alleles combinations

The following strains were used for this study:

UAS-Cherry::Tubulin (BDSC #25774), Ubi-RFP::Tubulin (gift from Renata Basto), UASt-mCherry::Jupiter (gift from Clemens Cabernard), UAS, His2Av::mRFP1 (BDSC #23651), His2Av::GFP[1] and GFP::Mad2[2] were used to monitor by live-imaging the microtubule network, chromosomes and unattached kinetochores. Wild-type (UASp-Polo^{WT}::GFP), phosphomutant (UASp-Polo^{T182A}::GFP), phosphomimic (UASp-Polo^{T182D}::GFP) and kinase-dead (UASp-Polo^{K54M}::GFP) Polo variants tagged with GFP were expressed using the Gal4-UAS system. All four constructs were inserted on the second chromosome (attP40, see below) and on the third chromosome (attP154,[3]).

Inscuteable-Gal4 (Insc-Gal4; BDSC #8751) and Worniu-Gal4 (Wor-Gal4; BDSC #56554) allowed the expression of UAS driven fluorescent markers in the neuroblasts; and Actin5C-Gal4 (BDSC #4414) was used for ubiquitous expression in somatic cells. The expression of Polo variants for protein level and rescue assays in Figure 2A and 2B as well as the expression of Polo^{T182D}::GFP for ploidy analysis (Figure 5E) were performed using the Actin5C-Gal4 driver. The expression of mCherry::Jupiter and Polo^{T182D}::GFP in *ial* mutant background were driven by Wor-Gal4. For other experiments (live-imaging, immunofluorescence and transplantation assay), Polo variants and the microtubule marker were expressed under the control of Insc-Gal4.

The following alleles were used in this study and described before: *aurA*^{8839} (referred as *aurA* mutant, [4,5]), *mad2*^{p} ([6]), *polo*^{1} ([7]), *polo*^{9} and *polo*^{10} ([8]), *ial*^{1689}, *ial*$^{35.33}$ and *ial*^{2A43} ([9]). The allelic combination *polo*^{9}/*polo*^{10} (referred as *polo* mutant) corresponds to a strong *polo* hypomorph mutant and the flies do not reach the pupal stage, as described before[10]. The allelic combinations *polo*^{1}/*polo*^{9} and *polo*^{1}/*polo*^{10} mutant flies are viable and corresponds to weak

26 *polo* hypomorph mutants[10]. The phenotype of Ial/Aurora B loss-of-function was assessed
27 during the larval stage using two heteroallelic combinations: $ial^{35.33}/ial^{1689}$ and ial^{2A43}/ial^{1689}.
28 Flies were maintained and crossed under standard conditions at 25°C.

29 **Generation of transgenes**

30 The constructs containing the coding sequence of Polo variants (WT, T182A, T182D and
31 K54M) C-terminally tagged with GFP were cloned into the plasmid pUAS-K10-attB[3] and
32 were injected in embryos for targeted insertion on the attP40 site located on second
33 chromosome (BestGene).

34 **Immunohistochemistry and antibodies**

35 Third instar larval brains (120 to 144 h after egg lying depending on overall growth delay)
36 were dissected in Schneider medium supplemented with 10% FCS and fixed in Testis Buffer
37 (183 mM KCl, 47 mM NaCl, 10 mM Tris, and 1 mM EDTA, pH 6.8) containing 10%
38 formaldehyde and 0.01% Triton X-100 at 25°C for 20 minutes, as described in a previous
39 study[11].

40 Primary antibodies: monoclonal anti-α-tubulin DM1A (mouse, 1:500, Sigma T6199), anti-
41 PKCζ (C-20) (rabbit, 1:250, Santa Cruz sc-216), anti-Miranda (rat, 1:200, Abcam 197788),
42 polyclonal anti-phosphorylated Ser10 of Histone H3 (rabbit, 1:500, Millipore 06-570) and
43 anti-Deadpan (rat, 1:200, Abcam 195172).

44 Secondary antibodies: anti-rat, anti-mouse and anti-rabbit conjugated to 488, 568, 647 Alexa-
45 Fluor (1:500 to 1:1000, Life Technologies).

46 Images were acquired on a Leica SP5 confocal microscope using 40X (1.25 N.A.) and 63X
47 (1.40 N.A.) objectives, controlled with Leica LAS software and analyzed on Fiji or Imaris.

48 **Western blotting and antibodies**

49 Two to three brains were dissected, resuspended in Laemmli Buffer and loaded on a 4-15%
50 Mini-PROTEAN TGX Precast Protein Gel (BioRad). After migration, proteins are transferred

51 on a nitrocellulose membrane using a Trans-Blot Turbo (BioRad). Membranes were washed
52 with PBS+0.1% Tween20 (PBST) and blocked with PBST+5 to 10% powder milk. The
53 membranes were then incubated in the following primary antibodies, diluted in TBST+2.5 to
54 5% powder milk: Rabbit polyclonal anti-Actin (I-19, Santa Cruz sc-1616-R; 1/4000), anti-
55 Mad2 (Gift from David Sharp; 1/500), mouse monoclonal anti-Polo MA294 (Gift from David
56 Glover; 1/100). Anti-mouse and anti-Rabbit secondary antibodies were purchased from
57 Jackson ImmunoResearch. Western blots were revealed with SuperSignal West Dura or
58 Femto (ThermoFisher).

59 **Live cell imaging**

60 Third instar larval brains (120 to 144h after egg lying depending on overall growth delay)
61 were dissected in Schneider medium containing 10% FCS and transferred to 50 µL wells
62 (Ibidi, µ-Slide Angiogenesis) for live imaging. Mutant and control brains were imaged in
63 parallel at 25°C. Z-series (thickness of 20 µm with 1 µm spacing) were acquired with a
64 temporal resolution of 30 to 90 s for 1 to 2.5 hours. Alternatively, samples were mounted on a
65 stainless-steel slide, between coverslip and mineral oil as described in a previous study[11].
66 Images were acquired with a spinning disk system consisting of a DMi8 microscope (Leica)
67 equipped with a 63X (1.4 N.A.) oil objective, a CSU-X1 spinning disk unit (Yokogawa) and
68 an Evolve EMCCD camera (Photometrics). The microscope was controlled by the Inscoper
69 Imaging Suite and the dedicated software (Inscoper). Alternatively, a CSU-X1 spinning-disk
70 unit mounted on an inverted microscope (Elipse Ti; Nikon) equipped with a 60X (1.4 N.A.)
71 oil objective, a sCMOS ORCA Flash 4.0 (Hamamatsu) and controlled by MetaMorph; was
72 also used for some experiments.
73 Images were processed with Fiji or Imaris softwares.

74 **Time in mitosis and spindle orientation angle measurements**

75 The time in mitosis was determined by the duration between NEBD (tubulin entry in the
76 nuclear space) and anaphase onset. Note that only the cells undergoing complete mitosis
77 within the span of the experiments were scored. For *ial;aurA* double mutant (Supplementary
78 Figure 2B-C) displaying the most severe phenotype, the cells could not complete mitosis
79 throughout the experiment (2.5 h) and the time in mitosis could not be measured. Spindle
80 orientation on fixed tissue was measured on metaphase cells using the "spot" tool of Imaris.
81 Briefly, two spots were placed in the center of the apical aPKC and basal Miranda crescents
82 to determine the polarity axis; two spots positioned at the spindle poles determined the mitotic
83 spindle axis. For *aurA* mutant that did not exhibit an apical aPKC crescent, the polarity axis
84 was determined by a straight line between the center of the Miranda crescent and a second
85 spot at the opposite cortex. The 3D coordinates of the spots were used to calculate polarity
86 and spindle axes vectors and the angle between them as described in [12].

87 **Ploidy analysis in brains**

88 Third instar larval brains were dissected in PBS, incubated for 8 minutes in 0.5% sodium
89 citrate solution, fixed in acetic acid (45% for 45 seconds and 60% for 2 minutes), squashed
90 between slide and coverslip and flash-frozen in liquid nitrogen (Caous et al., 2015). After
91 coverslip flip off, the squashed cells on the slide were washed in PBS and mounted in
92 ProlonGold supplemented with DAPI. Images were acquired using a Leica DMRXA2
93 microscope equipped a 63X (1.32 N.A.) objective, a CoolSnap HQ2 camera and controlled by
94 MetaMorph. Images were processed with Fiji software.

95 **Tumor transplantation assay**

96 The protocol to assess proliferation ability of brain tissues was originally set up in the lab of
97 Cayetano Gonzalez[13]. Briefly, a central brain fragment (expressing a fluorescent probe) was
98 transplanted in the abdomen of a live wild-type adult female fly and the growth of the
99 transplant was monitored over time. Control or mutant third instar larval brains, expressing

either His2Av::GFP or UAS-Cherry::Tubulin under the control of Insc-Gal4 were dissected in sterile PBS (Sigma). One brain lobe was transplanted in the abdomen of a wild-type adult fly using a pulled capillary with a beveled tip (around 150 µm diameter) adjusted to a microinjection system (IM-9B; Narishige). After transplantation, host flies were maintained at 18°C overnight and transferred at 25°C for a month. Tumor growth was monitored every one or two days upon 30 days for the appearance of a mCherry or GFP signal in the abdomen. For *aurA* and strong *polo* mutants, transplant growth was assessed over a 15-days period because these tumors were particularly aggressive and killed the host flies before 30 days. The neuroblast-specific Insc-Gal4 was used to assay the effect of $Polo^{T182D}$::GFP variant for tumor growth.

Statistical analyses

Sample size and statistical test used for each analysis are found in the corresponding figure legends. Statistical analyses were performed using the Prism software (Version 7, GraphPad). Two tests were used according to the data: to compare ranks between two unpaired samples with variable variances and non-Gaussian distributions, a nonparametric Mann-Whitney test was used; while the comparisons of proportions were assessed by a two-sided Fisher's exact test with a confidence index of 95%. Significance are displayed on the figure: ns: $p>0.05$; *: $p<0.05$; **: $p<0.01$; ***: $p<0.001$; ****: $p<0.0001$.

References

1. Clarkson, M. & Saint, R. A His2AvDGFP Fusion Gene Complements a Lethal His2AvD Mutant Allele and Provides an in Vivo Marker for Drosophila Chromosome Behavior. *DNA Cell Biol.* **18**, 457–462 (1999).
2. Buffin, E., Lefebvre, C., Huang, J., Gagou, M. E. & Karess, R. E. Recruitment of Mad2 to the Kinetochore Requires the Rod/Zw10 Complex. *Curr. Biol.* **15**, 856–861 (2005).
3. Kachaner, D. *et al.* Coupling of Polo kinase activation to nuclear localization by a bifunctional NLS is required during mitotic entry. *Nat. Commun.* **8**, (2017).
4. Wang, H. *et al.* Aurora-A acts as a tumor suppressor and regulates self-renewal of Drosophila neuroblasts. *Genes Dev.* **20**, 3453–3463 (2006).

5. Lee, C.-Y. *et al.* Drosophila Aurora-A kinase inhibits neuroblast self-renewal by regulating aPKC/Numb cortical polarity and spindle orientation. *Genes Dev.* **20**, 3464–3474 (2006).
6. Buffin, E., Emre, D. & Karess, R. E. Flies without a spindle checkpoint. *Nat. Cell Biol.* **9**, 565–572 (2007).
7. Sunkel, C. E. & Glover, D. M. polo, a mitotic mutant of Drosophila displaying abnormal spindle poles. *J. Cell Sci.* **89**, (1988).
8. Donaldson, M. M., Tavares, Á. A. M., Ohkura, H., Deak, P. & Glover, D. M. Metaphase Arrest with Centromere Separation in polo Mutants of Drosophila. *J. Cell Biol.* **153**, 663–676 (2001).
9. Mathieu, J. *et al.* Aurora B and Cyclin B Have Opposite Effects on the Timing of Cytokinesis Abscission in Drosophila Germ Cells and in Vertebrate Somatic Cells. *Dev. Cell* **26**, 250–265 (2013).
10. Carmena, M., Lombardia, M. O., Ogawa, H. & Earnshaw, W. C. Polo kinase regulates the localization and activity of the chromosomal passenger complex in meiosis and mitosis in *Drosophila melanogaster*. *Open Biol.* **4**, 140162 (2014).
11. Gallaud, E. *et al.* Ensconsin/Map7 promotes microtubule growth and centrosome separation in Drosophila neural stem cells. *J. Cell Biol.* **204**, 1111–1121 (2014).
12. Loyer, N. The last-born daughter cell contributes to division orientation of Drosophila larval neuroblasts. *Nat. Commun.* 12 (2018).
13. Caussinus, E. & Gonzalez, C. Induction of tumor growth by altered stem-cell asymmetric division in Drosophila melanogaster. *Nat. Genet.* **37**, 1125–1129 (2005).